Electronic Supplementary Material (ESI) for Materials Chemistry Frontiers.
This journal is © the Partner Organisations 2021

Supplementary information for

Atomic Fe–N_5 Catalytic Site Embedded in N-doped Carbon as Highly Efficient Oxygen Electrocatalyst for Zinc–Air Batteries

Huinian Zhang*, Suping Jia, Xiaolin Shi, Ziyuan Li, Bin Liu, Ning Li, Ying Li, Shengliang Hu and Huiqi Wang*

School of Energy and Power Engineering, North University of China, Taiyuan 030051, P. R. China.

E-mail: zhanghuinian123@163.com (Huinian Zhang);

hqiwang@163.com (Huiqi Wang)

ABSTRACT

Atomically dispersed transition metal–N_x–C-based catalysts with abundant Fe–N_x active sites have demonstrated good prospects for oxygen-reduction reaction (ORR) and are promising alternatives to Pt-based electrocatalysts. However, further improving their ORR activity by precise modulation of the Fe–N_x site structure remains challenging. Herein, we synthesize a single-iron-atom electrocatalyst embedded in N-doped carbon with active and robust five-coordinated Fe–N_5 moieties by a simple synthetic approach. The FeN_5-C/G catalyst is obtained through prolonged calcination of melamine and hemin co-adsorbed on oxide graphene. The catalyst exhibits an enhanced ORR activity in alkaline mediums with an admirable half-wave potential of 0.84 V, outperforming FeN_4-C, which has four-coordinated Fe–N_4 moieties. Zn–air batteries with FeN_5-C/G air cathode further demonstrates excellent ORR performance and stability of the catalyst, outperforming the commercial Pt/C catalyst. The remarkable ORR performance demonstrates the significant roles of mono-dispersed

FeN$_5$ active sites embedded in N-doped carbon, in which N-doped graphene supplies enough N sites to axially coordinate with FeN$_4$.

Keywords

single-atom electrocatalyst, Fe–N$_5$ active site, oxygen reduction reaction, hemin, Zn–air battery

Additional Figures

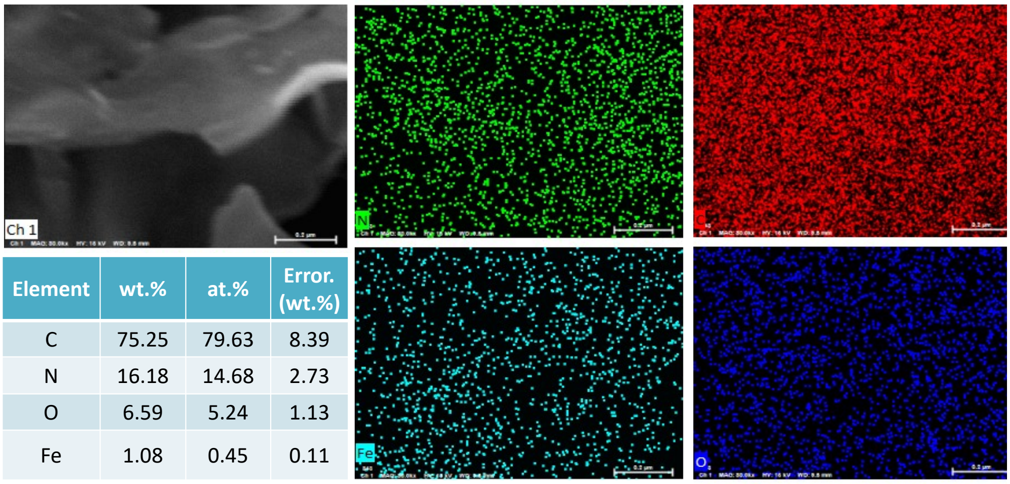

Element	wt.%	at.%	Error. (wt.%)
C	75.25	79.63	8.39
N	16.18	14.68	2.73
O	6.59	5.24	1.13
Fe	1.08	0.45	0.11

Figure S1 SEM, EDS and correspondingly quantified elemental percentage of the FeN$_5$-C/G catalyst.

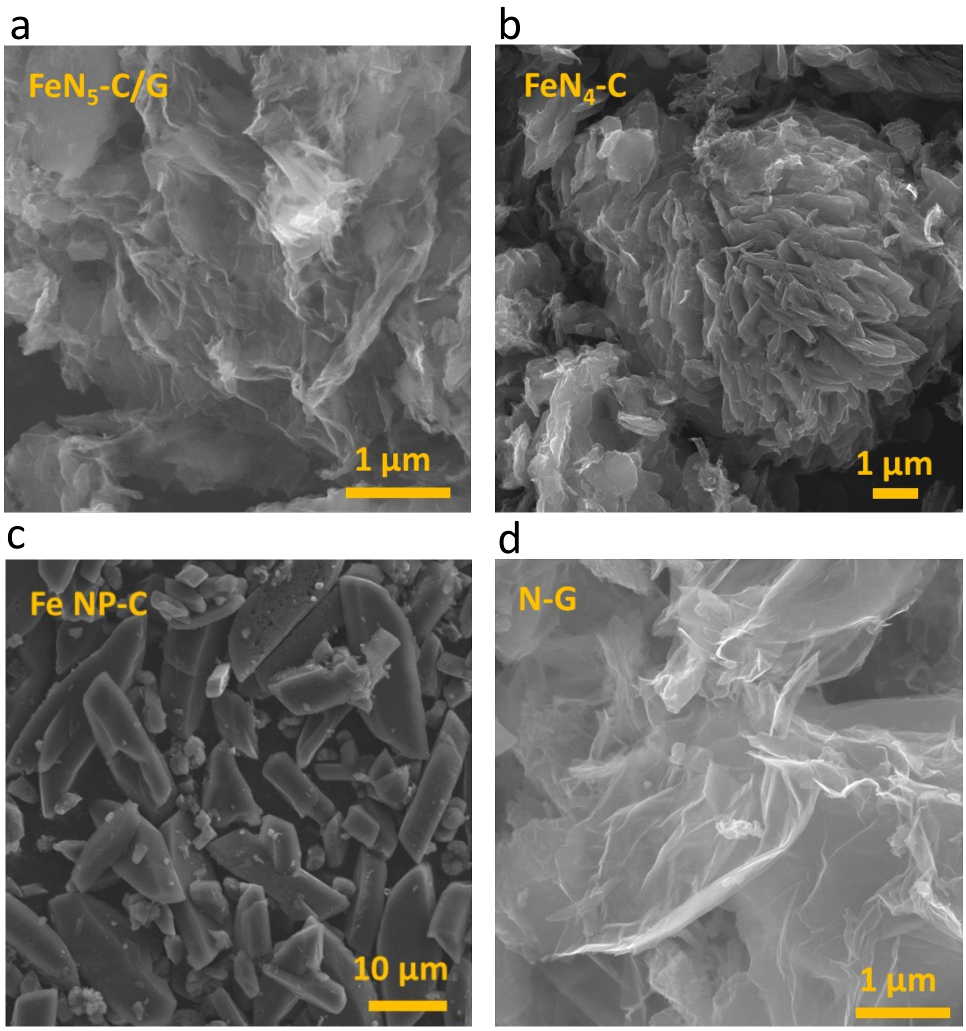

Figure S2 SEM images of different catalysts: (a) FeN_5-C/G catalyst, (b) FeN_4-C catalyst, (c) Fe NP-C catalyst and (d) N-G catalyst.

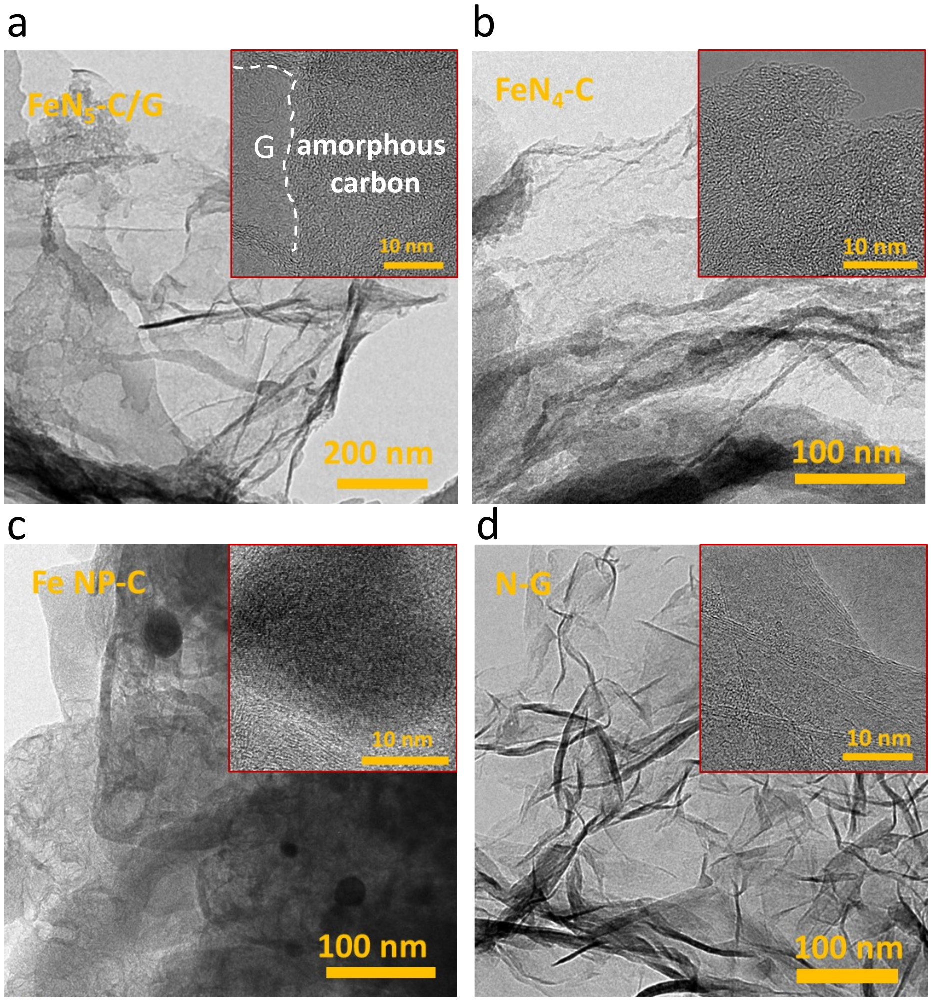

Figure S3 TEM (inset: HR-TEM) images of different catalysts: (a) FeN_5-C/G catalyst, (b) FeN_4-C catalyst, (c) Fe NP-C catalyst and (d) N-G catalyst.

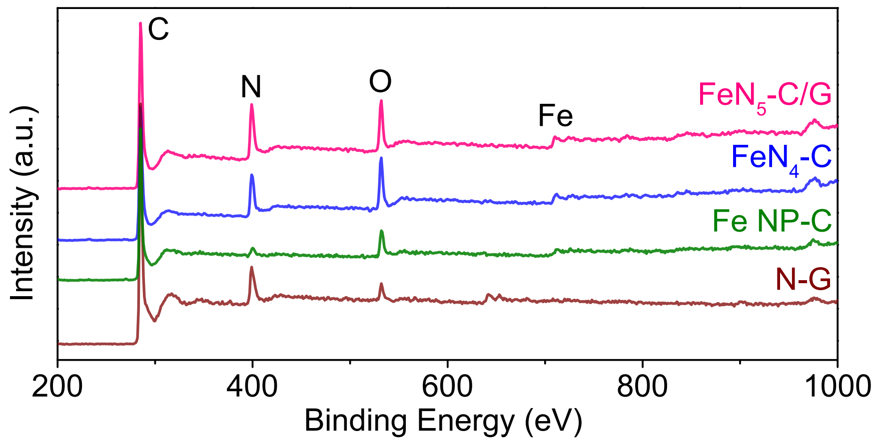

Figure S4 XPS full spectra of FeN_5-C/G catalyst compared to FeN_4-C, N-G and Fe NP-C.

Table S1 Atomic ratios (at. %) of O, Fe, N and C elements in FeN_5-C/G, FeN_4-C, N-G and Fe NP-C catalysts based on XPS analysis.

Sample	C content (at%)	N content (at%)	Fe content (at%)	O content (at%)
N-G	86.08%	11.47%	-	2.45%
FeN_5-C/G	74.11%	15.86%	1.40%	8.63%
FeN_4-C	71.78%	16.02%	1.24%	10.97%
Fe NP-C	86.80%	5.37%	0.59%	7.24%

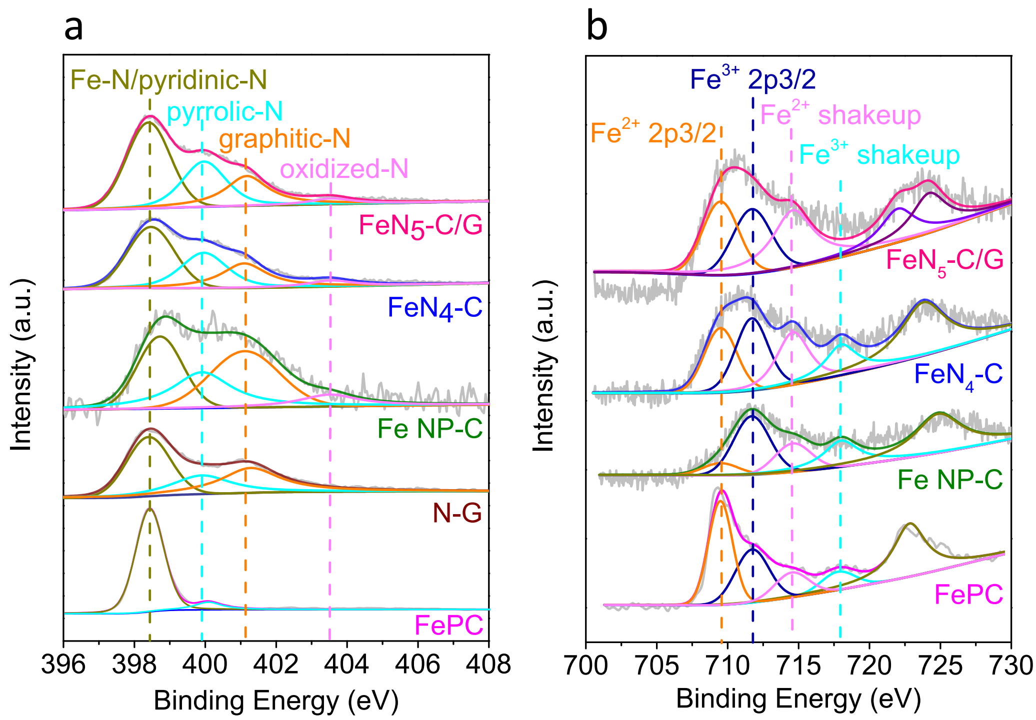

Figure S5 XPS spectra of FeN_5-C/G catalyst compared with control samples. (a) XPS spectra of N1s peaks with the deconvolution, (b) XPS spectra of Fe2p peaks with the deconvolution.

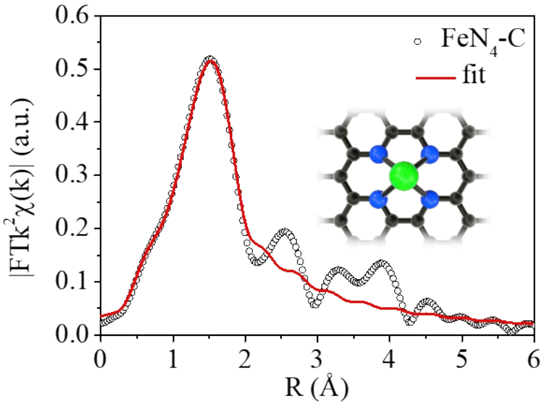

Figure S6 EXAFS-fitting curves at R space of FeN$_4$-C with Fe–N$_4$ model.

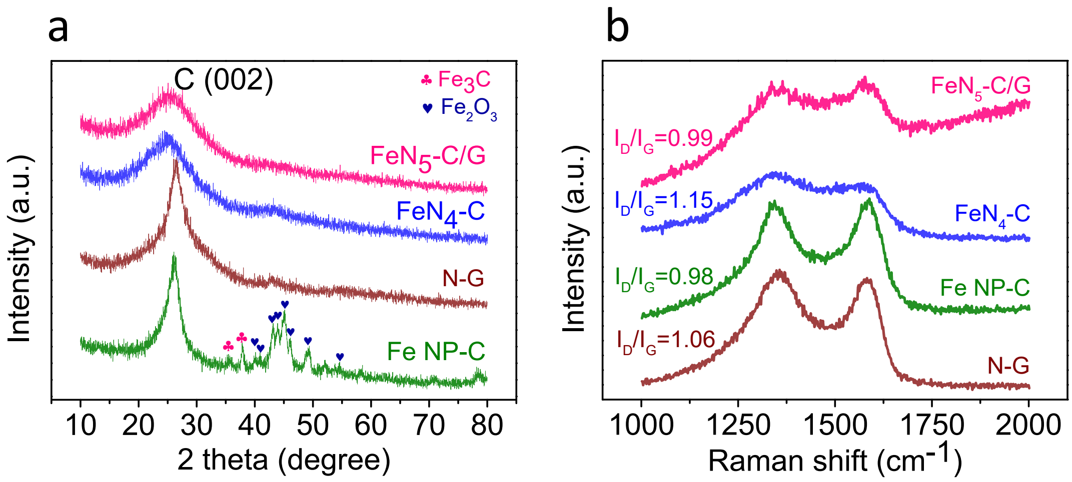

Figure S7 (a) XRD spectra and (b) Raman spectra of FeN$_5$-C/G compared with FeN$_4$-C, Fe NP-C and N-G samples.

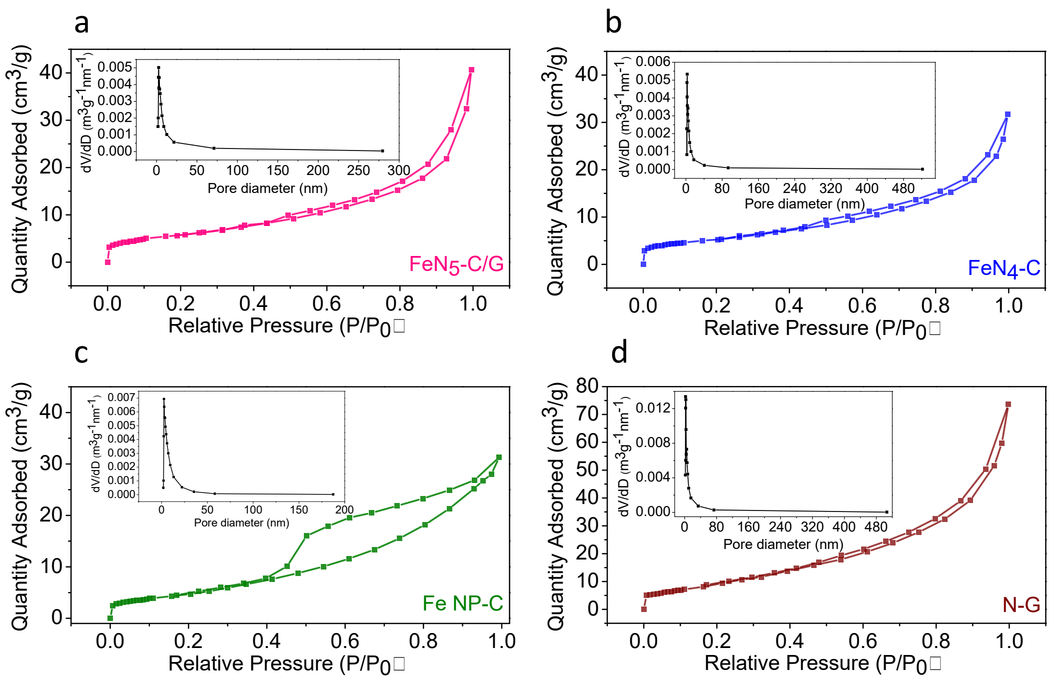

Figure S8 N_2 adsorption-desorption isotherm (inset: pore size distribution) of FeN_5-C/G compared with FeN_4-C, N-G and Fe NP-C catalysts.

Table S2 The size and volume distribution of the pores for the FeN_5-C/G catalyst compared with FeN_4-C, N-G and Fe NP-C catalysts.

Sample	S_{BET} (m^2/g)	V_{total} (cm^3/g)	V_{meso} (cm^3/g)	V_{micro} (cm^3/g)	V_{micro} /V_{total}	D (nm)
FeN_5-C/G	21	0.063	0.0552	0.0078	12%	12.046
FeN_4-C	19	0.049	0.0418	0.0072	15%	10.398
N-G	36	0.114	0.1029	0.0111	9.7%	12.607
Fe NP-C	18	0.048	0.0419	0.0061	13%	10.873

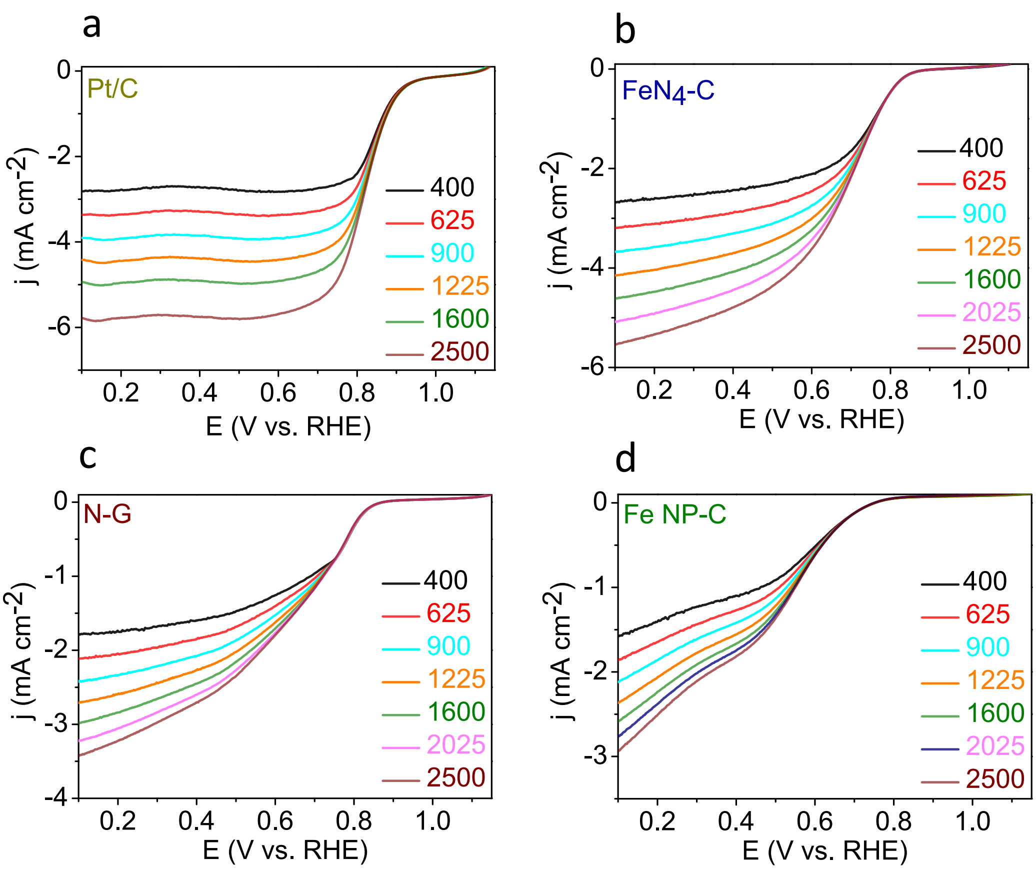

Figure S9 LSV curves of various catalysts with various rotation rates (a) Pt/C, (b) FeN_4-C, (c) N-G and (d) Fe NP-C.

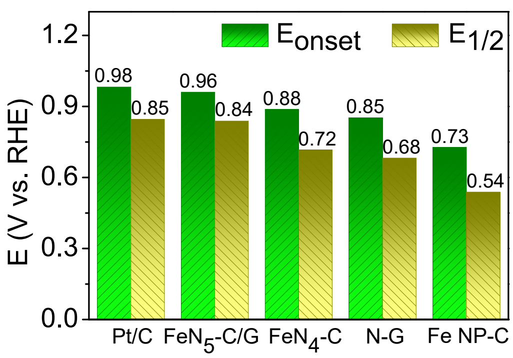

Figure S10 Onset potentials (E_{onset}) and half-wave potentials ($E_{1/2}$) of Pt/C, FeN_5-C/G, FeN_4-C, N-G and Fe NP-C catalysts.

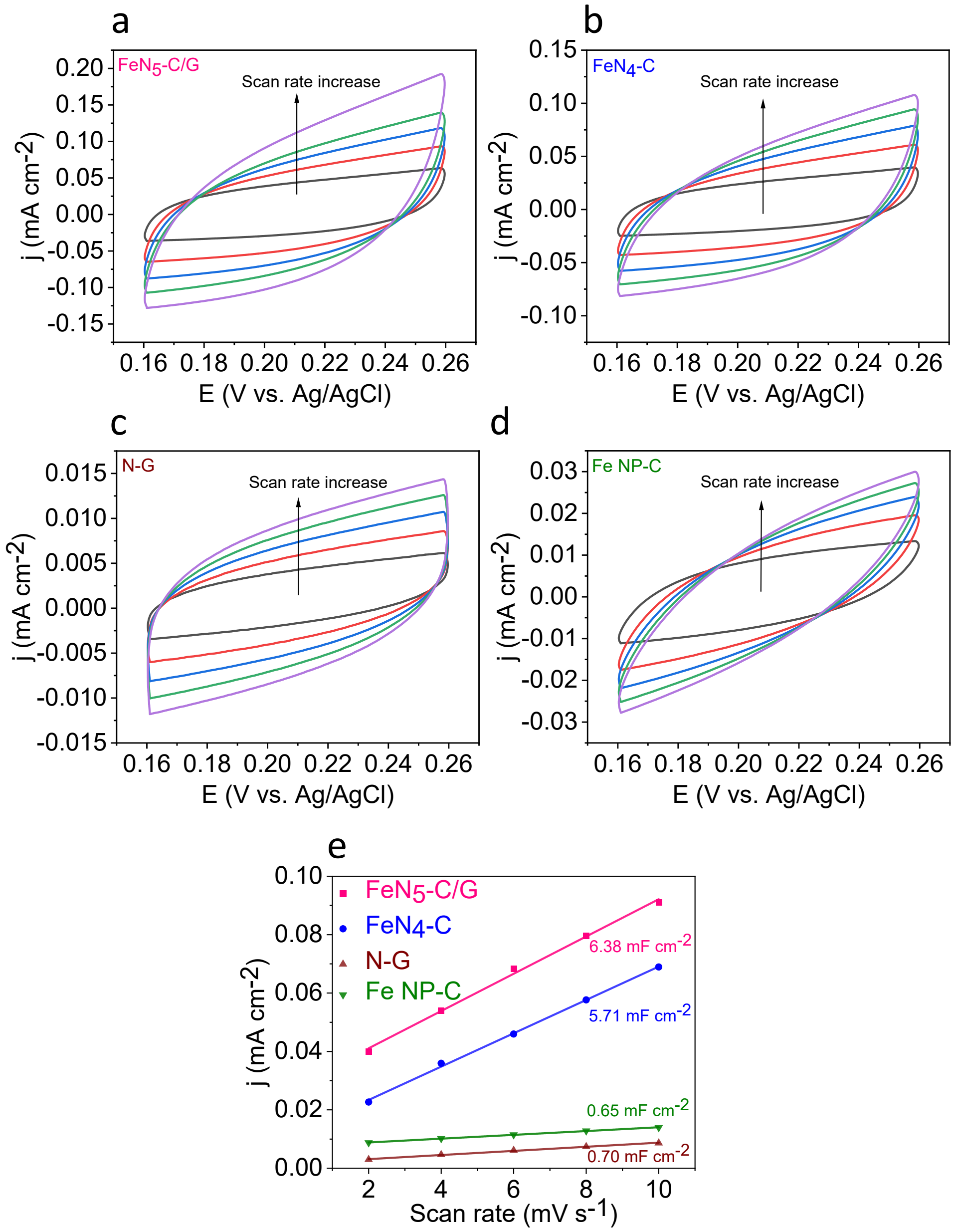

Figure S11 CV curves at different scan rates (2, 4, 6, 8, 10 mV/s) of (a) FeN_5-C/G and (b) FeN_4-C, (c) N-G, (d) Fe NP-C. (e) C_{dl} calculations of FeN_5-C/G and FeN_4-C.

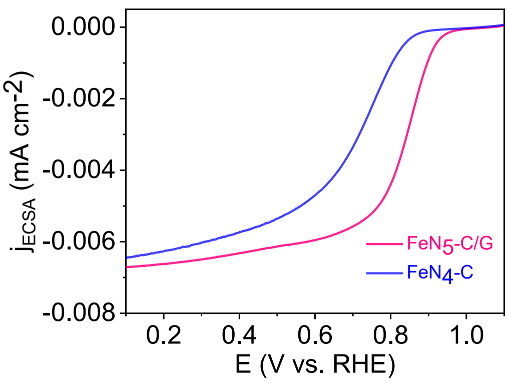

Figure S12 ECSA normalized LSV curves of FeN_5-C/G and FeN_4-C.